DMD Fast Forward. Published on October 22, 2019 as DOI: 10.1124/dmd.119.089268
This article has not been copyedited and formatted. The final version may differ from this version.

Numerical Analysis of Time Dependent Inhibition by MDMA of CYP2D6

John T. Rodgers, and Jeffrey P. Jones*

Department of Chemistry, Washington State University, Pullman, WA 99164

*Corresponding author: E-mail address: jpj@wsu.edu

DMD Fast Forward. Published on October 22, 2019 as DOI: 10.1124/dmd.119.089268
This article has not been copyedited and formatted. The final version may differ from this version.

Running Title: Numerical Analysis of Time Dependent Inhibition by MDMA of CYP2D6

Corresponding Author: Jeffrey P. Jones, PhD
Department of Chemistry
Washington State University
Pullman, WA 99164-4630

Ph: (509)592-8790

jpj@wsu.edu

Number of text pages: 35

Number of tables: 3

Number of figures: 5

Number of references: 31

Number of words in Abstract: 206

Number of words in Introduction: 722

Number of words in Discussion: 987

List of Abbreviations: AICc - corrected Akaike information criterion

CYP - cytochrome P450

DDI - drug-drug interaction

DEM - dead enzyme model

DHMA - dihydroxymethamphetamine

EM - equilibrium model

HLM - human liver microsomes

MAM - modified activity model

MDA - methylenedioxyamphetamine

MDMA - methylenedioxymethamphetamine

MDP - methylenedioxyphenyl

DMD Fast Forward. Published on October 22, 2019 as DOI: 10.1124/dmd.119.089268
This article has not been copyedited and formatted. The final version may differ from this version.

MIC - metabolic intermediate complex

PRA - percent remaining activity

QI - quasi-irreversible

TDI - time dependent inhibition

DMD Fast Forward. Published on October 22, 2019 as DOI: 10.1124/dmd.119.089268
This article has not been copyedited and formatted. The final version may differ from this version.

Abstract

Methylenedioxymethamphetamine (MDMA) is a known drug of abuse and schedule 1 narcotic under the Controlled Substances Act. Previous pharmacokinetic work on MDMA used classical linearization techniques to conclude irreversible mechanism-based inhibition of CYP2D6. The current work challenges this outcome by assessing the possibility of two alternative reversible kinetic mechanisms known as the quasi-irreversible (QI) and equilibrium (EM) inhibition models. In addition, progress curve experiments were used to investigate the residual metabolism of MDMA by liver microsomes and 2D6 baculosomes over incubation periods up to 30 minutes. These experiments revealed activity in a terminal linear phase at the fractional rates with respect to initial turnover of 0.0354 ± 0.0089 in HLM and 0.0114 ± 0.0025 in baculosomes. Numerical model fits to percent-remaining-activity (PRA) data were consistent with progress curve modeling results, wherein an irreversible inhibition pathway was found unnecessary for good fit scoring. Both QI and EM kinetic mechanisms fit the PRA data well, although in 2D6 baculosomes the inclusion of an irreversible inactivation pathway did not allow for convergence to a reasonable fit. The kinetic complexity accessible to numerical modeling has been used to determine that MDMA is not an irreversible inactivator of CYP2D6, and instead follows what can be generally referred to as slowly reversible inhibition.

DMD Fast Forward. Published on October 22, 2019 as DOI: 10.1124/dmd.119.089268
This article has not been copyedited and formatted. The final version may differ from this version.

Significance Statement

The work herein describes usage of computational models to delineate between irreversible and slowly reversible time dependent inhibition. Such models are used in the paper to analyze MDMA and classify it as a reversible time dependent inhibitor which will lead to recovery of CYP 2D6 activity in less than half the time of an irreversible inhibitor.

DMD Fast Forward. Published on October 22, 2019 as DOI: 10.1124/dmd.119.089268
This article has not been copyedited and formatted. The final version may differ from this version.

Introduction

Cytochromes P450 comprise a superfamily of enzymes known for their promiscuous oxidative catalysis. With a predominant role in phase 1 metabolism, these enzymes have been a focal point for first pass kinetics and drug-drug interaction (DDI) analyses (Soars *et al.*, 2007; Zanger and Schwab, 2013). Efforts to produce new therapeutics are therefore dependent on accurate correspondence between in vitro predictions and in vivo outcomes. Some of the most difficult *in vitro* to *in vivo* predictions include DDIs stemming from time dependent inhibition (TDI), which results in accumulation of inactive enzyme over time (Silverman, 1995). Time dependent inhibition is historically attributed to a covalent modification of a protein by an inhibitor, resulting in an irreversible (or quasi-irreversible) and inactive metabolic intermediate complex (MIC) (Wienkers and Heath, 2005; Takakusa *et al.*, 2011; Orr *et al.*, 2012). Techniques to parameterize TDI are numerous, though experimental and analytical methods regarding *in vivo* TDI prediction have been topics of disagreement among pharmacokineticists, with FDA guidances providing limited success (Atkinson *et al.*, 2005; Grimm *et al.*, 2009; VandenBrink and Isoherranen, 2010; Burt *et al.*, 2012).

Disagreement between in vitro predictions and in vivo outcomes has been attributed, in part, to the steady-state assumptions inherent to the replot method: the FDA-supported TDI data analysis methodology. Restricted to irreversible and Michaelis-Menten kinetic models, the replot method tends to fail as semi-log percent-remaining-activity (PRA) plots become nonlinear (Nagar *et al.*, 2014). The impact of this insufficiency has materialized in that TDI preincubations have been truncated to include only the log-linear inactivation phases where inactivation is rapid; this has been associated with a systematic overprediction of K_I (Korzekwa *et al.*, 2014; Barnaba *et al.*, 2016; Yadav *et al.*, 2018). Tools created to account for non-linear kinetics have been developed

DMD Fast Forward. Published on October 22, 2019 as DOI: 10.1124/dmd.119.089268
This article has not been copyedited and formatted. The final version may differ from this version.

to overcome this phenomenon (Cleland, 1975; Cao *et al.*, 2013). Recently, a numerical curve fitting method that opts for a rapid equilibrium assumption in place of the steady state assumption has garnered attention due to its ability to evaluate complex kinetic behavior including multi-inhibitor binding, and partial and quasi-irreversible inactivation (Korzekwa *et al.*, 2014). With increasing prevalence of non-linear and numerical curve fitting algorithms, the space for new kinetic models has widened considerably.

Substrates containing alkylamines, hydrazines, or methylenedioxyphenyl (MDP) groups have been associated with MIC formation, and therefore time dependent inhibition, in the 3A4 and 2D6 P450 isoenzymes. Podophyllotoxin, an MDP-containing therapeutic, has been classified as a quasi-irreversible inhibitor of P450 3A4, for example (Barnaba *et al.*, 2016). Quasi-irreversible TDI is characterized by formation of a slowly reversible MIC that occurs as a result of complexation by a reactive intermediate to the heme's ferrous iron (Orr *et al.*, 2012). Oxidation of MDPs to carbene groups facilitates this complexation. A separate, studied example of a xenobiotic containing the MDP moiety is methylenedixoymethamphetamine (MDMA).

MDMA is a drug of abuse known for its entactogenic properties, and has been associated with severe effects as well as potential drug-drug interactions (Dowling *et al.*, 1987; Screaton *et al.*, 1992; Harrington *et al.*, 1999). MDMA is metabolized in parallel by CYPs 3A4, 1A2, 2C19, 2B6, and with high affinity for 2D6 to the demethylenated and N-demethylated metabolites dihydroxymethamphetamine (DHMA) and methylenedioxyamphetamine (MDA), respectively (Meyer *et al.*, 2008). Phase II reactions are facilitated by catechol-O-methyl-transferase (de la Torre *et al.*, 2004), glucuronidation (Bastos *et al.*, 2004), or sulfation (Antolino-Lobo *et al.*, 2011). MDMA is a reported time dependent inhibitor of CYP2D6 (A. Heydari, K. Rowland Yeo, M. S. Lennard, S. W. Ellis, G. T. Tucker, 2004; Van *et al.*, 2006, 2007). Characterization of

DMD Fast Forward. Published on October 22, 2019 as DOI: 10.1124/dmd.119.089268
This article has not been copyedited and formatted. The final version may differ from this version.

MDMA's TDI potency was published by Heydari et al (2006), wherein preincubation times up to 5 minutes were used with the replot method to establish k_{inact} and K_I values of 0.29 ± 0.03 min^{-1} and 12.9 ± 3.6 µM in yeast microsomes. The same publication reported inactivation parameter estimates for three human liver samples which estimated K_I values in the range of 8.8 to 45.3 µM, and k_{inact} values in the range of 0.12 to 0.26 min^{-1}. It is the belief of the authors of that additional information about the inhibition of 2D6 by MDMA can be extracted by examining data beyond this preincubation time range. The goal of the current study is to use a numerical computational technique to facilitate a more accurate parameterization of MDMA's time dependent inactivation in recombinant 2D6 and microsomal systems.

DMD Fast Forward. Published on October 22, 2019 as DOI: 10.1124/dmd.119.089268
This article has not been copyedited and formatted. The final version may differ from this version.

Methods and Materials

Materials

Baculosomes expressing 2D6 were obtained from Invitrogen Corp. (Carlsbad, CA), and human liver microsomes (HLM) pooled from 50 donors of mixed gender were purchased from Gibco (Austin, TX). Catalase, dextromethorphan, and methylenedioxymethampthetamine were obtained from Sigma-Aldrich (St. Louis, MO), and tris(2-carboxyethyl) phosphine (TCEP) was purchased from Goldbio (St. Louis, MO). Superoxide dismutase and NADPH were purchased from EMD Millipore Corp. (Billerica, MA), and EMD Chemicals (San Diego, CA), respectively. MDMA metabolites used for LCMS method development were purchased from Cayman Chemical (Ann Arbor, MI).

Progress Curve Assays

Metabolism over time was measured using a saturating MDMA concentration (50uM). A buffer mix containing 0.5mM EDTA, 2mM TCEP, 125u/mL catalase and 0.1M potassium phosphate was preincubated with human liver microsomes (0.2mg/mL) or recombinant 2D6 (10nM) for 5 minutes before addition of NADPH to a final concentration of 1mM. At 11 time points (0-60 minutes) aliquots were removed into an ice-cold quench solution containing 25µM phenacetin and 1M formic acid.

Time Dependent Inhibition Assays

Samples in the preincubation phase contained human liver microsomes (0.2mg/mL) or 2D6 baculosomes (10nM), MDMA (0-20µM), superoxide dismutase and catalase (125u/mL each), and potassium phosphate (0.1M, pH 7.4). Upon activation by NADPH (1mM), samples were preincubated for 0-30 minutes before a 10-fold dilution with probe solution containing

DMD Fast Forward. Published on October 22, 2019 as DOI: 10.1124/dmd.119.089268
This article has not been copyedited and formatted. The final version may differ from this version.

superoxide dismutase and catalase (125 u/mL), NADPH (1mM), and a saturating concentration of dextromethorphan (50µM) to probe remaining activity. Diluted samples were further incubated for 7 minutes. The reaction was stopped with 25% sample volume of ice-cold quench containing 1M formic acid in acetonitrile as well as a known amount of phenacetin to be used as internal standard. Quenched samples were centrifuged for 10 minutes at 10,000rcf.

LC-MS/MS

Metabolite quantification was achieved using an LC-20AD series high performance liquid chromatography system (Shimadzu, Columbia, MD) fitted with an HTC PAL autosampler (LEAP Technologies, Carrboro, NC). For TDI samples, chromatography was performed on a Luna C18 column (50 x 2.0mm, 5µm; Phenomenex, Torrance, CA); DHMA quantitation necessitated a Synergi C18 column (250 x 4.6mm, 4µm; Phenomenex, Torrance, CA). Solvent gradients occurred in two mobile phases: mobile phase A consisted of 0.05% formic acid and 0.2% acetic acid in water, and mobile phase B was comprised of 0.1% formic acid, 9.9% water, and 90% acetonitrile. For dextrorphan, an initial condition of 90% mobile phase A was held constant at 0.4mL/min for 0.3 minutes. Separation was achieved over 1.9 minutes with a linear gradient to 25% mobile phase A, which was held constant for an additional 0.1 minutes. The column was then re-equilibrated to initial conditions over the final 1.7 minutes of the 4-minute program. A unique 4-minute program was used to achieve separation of methylenedioxyampehtmaine, wherein an initial condition of 90% mobile phase A was held for 1 minute at 0.4mL/min before a 1.5-minute linear gradient to 25% mobile phase A, which was maintained for 0.5 minutes. The column was then equilibrated to initial conditions over the final 1.5 minutes.

DMD Fast Forward. Published on October 22, 2019 as DOI: 10.1124/dmd.119.089268
This article has not been copyedited and formatted. The final version may differ from this version.

The dihydroxy metabolite of MDMA required a 16-minute chromatographic separation. An initial condition of 95% mobile phase A was maintained for 1 minute before separation was achieved with a linear gradient to 5% mobile phase A over 7 minutes. This condition was maintained for 4 minutes before equilibrating to the initial condition over the final 4 minutes. Metabolites were measured using multi-reaction monitoring mode with the following mass fragment transitions: dextrorphan (258.18/201.10), DHMA (182.10/105.00), MDA (180.20/163.20), phenacetin (180.20/110.10).

Ionization tuning parameters with the exception of collision energy remained consistent for all quantitation and were as follows: curtain gas, 20; ion spray voltage, 4900; ion source gas 1, 35.0; ion source gas 2, 55.0; temperature, 400.0; declustering potential, 55.0; entrance potential, 10.0; collision cell exit potential, 10.0. A collision energy of 50.0 was used for dextrorphan, and 35.0 for DHMA.

Data Analysis

Time-dependent inhibition data were first fit using a standard replot of natural log percent-remaining-activity vs inhibitor concentration. Replots were created for abbreviated sets restricted to include only log-linear inactivation data. Fitting protocols accounting for the curved nature of MDMA TDI necessitated the development of a kinetic model defined by numerical methods described previously (Korzekwa *et al.*, 2014; Nagar *et al.*, 2014). Two numerical mechanisms were built in accordance with previous work (Abbasi *et al.*, 2019) to model nonlinear metabolite production; these models (Modified Activity and Dead Enzyme) were fit to an MDMA progress curve for initial inactivation assessment.

DMD Fast Forward. Published on October 22, 2019 as DOI: 10.1124/dmd.119.089268
This article has not been copyedited and formatted. The final version may differ from this version.

Two larger numerical models were built to test the irreversibility of inactivation as well as possible kinetic mechanisms of reversibility for full TDI experiments (having both inhibition and probe substrate turnover pathways). Model fitting was achieved with Mathematica 11.0 (Wolfram Research, Champagne, IL). Differential equations were evaluated using the NonLinearModelFit function with a precision goal of 12, and with 10000 max iterations. Dextromethorphan (S) and MDMA (I) binding rate constants (k_1, and k_4, respectively) were fixed at 270μM s^{-1}. Dissociation rate constants for were fixed at 2000μM s^{-1} (DXM) and 2970μM s^{-1} (MDMA) to reflect experimentally determined net rates. The concentration of 2D6 in liver microsomes was estimated to be 50nM based on the manufacturer's specification of total P450 concentration as well as a report of CYP2D6 representation among hepatic P450s (Michaels and Wang, 2014). Numerical fitting results were evaluated according to AICc, R^2, correlation matrices, and residuals plots.

DMD Fast Forward. Published on October 22, 2019 as DOI: 10.1124/dmd.119.089268
This article has not been copyedited and formatted. The final version may differ from this version.

Results

Progress Curve Kinetics

Production of the dihydroxy product of MDMA was observed to have a short steady-state range, becoming nonlinear within 5 minutes of incubation. Here, the modified activity model (MAM) and Dead Enzyme Model (DEM) reported by Abbasi and coworkers (2019) were used to parameterize curves beyond the steady-state range (Figure 1). In liver microsomes the MAM solved for an initial turnover rate (k_3) of 13.0 min^{-1} with a transition via k_4 (0.721 min^{-1}) to the slower terminal rate (k_5) of 0.461 min^{-1}. The DEM computed a single turnover rate of 10.4 min^{-1} with an irreversible inactivation rate of 0.448 min^{-1}. Though both models parameterized the data well, the fit scoring of the MAM slightly outperformed that of the DEM with an AICc of -225.9 vs -215.7, respectively (Table 1). A similar experiment in recombinant 2D6 agreed with the incomplete inhibition observed in microsomes. The 2D6 progress curves were better fit by the MAM (AICc -115.6) than the DEM (AICc -94.6). For the MAM, an inactivation constant analogous to k_{inact} can be obtained as the ratio of k_5 to k_3, which describes the fractional residual activity of the terminal phase with respect to the initial rate. Using this ratio, residual activities were calculated to be 0.0354 ± 0.0089 in HLM and 0.0114 ± 0.0025 in baculosomes.

PRA Replot Method

Given the nonlinearity of the data, the dataset was necessarily truncated for this steady-state analysis. The traditional inactivation rate replot method was applied to the linear range of percent-remaining-activity points. The rapid deviation from linearity in 2D6 baculosomes required that the data be truncated to the minimum three points. Slopes were replot against inhibitor concentration and fit according to the steady-state equation:

DMD Fast Forward. Published on October 22, 2019 as DOI: 10.1124/dmd.119.089268
This article has not been copyedited and formatted. The final version may differ from this version.

$$k_{obs} = \frac{k_{inact}[I]}{K_I + [I]}$$

in which k_{obs} is the negative of the slope of the linear inactivation rate, k_{inact} is the maximal inactivation rate (the horizontal asymptote of the replot hyperbola), K_I is the inhibitor concentration at which half-maximal inactivation occurs, and I is the inhibitor concentration. Fit of the steady state model to the replot data (Figure 2) yielded k_{inact} and K_I values of 0.246 ± 0.017 min^{-1} and 4.19 ± 0.77 μM in human liver microsomes. In recombinant 2D6, k_{inact} was fit to 0.309 ± 0.008 min^{-1} and K_I to 0.195 ± 0.043 μM.

Numerical TDI Models

Kinetic mechanisms were constructed to test the reversibility of inactivation. Two reversible model scaffolds were hypothesized based in part on previously reported mechanisms (Figure 3). Both numerical models consisted of an inhibitor-independent inactivation rate (k_8) to account for the nonspecific activity loss as a function of preincubation time, as was observed in each of the 0μM MDMA PRA plots. The first mechanism was informed by work on MDP inactivation of 3A4 (Barnaba *et al.*, 2016). Here, quasi-irreversible (QI) inactivation (k_9) and recovery (k_7) pathways partition from the reactive intermediate complex (E2). This mechanism was tested with and without the k_9 pathway in order to compare fit scoring in the presence and absence of irreversible inactivation. In HLM (Figure 4), both QI models with and without k_9 fit indistinguishably (AICC -242.2 and -241.1, respectively), while in 2D6 baculosomes only the model absent of an irreversible inhibition pathway was able to converge on positive rate constant solutions (Table 2).

A second mechanism with a reversible inactivation event, the equilibrium model (EM), was hypothesized based on our previous spectral work suggesting that MDMA is a true reversible

DMD Fast Forward. Published on October 22, 2019 as DOI: 10.1124/dmd.119.089268
This article has not been copyedited and formatted. The final version may differ from this version.

inhibitor in recombinant 2D6 (Rodgers *et al.*, 2018). Again, the k_9 pathway was manipulated to test the propensity for irreversible inactivation of the protein. Similar to the QI model, in HLM the presence of k_9 yielded indistinguishable differences in the overall fit (AICC -242.0 with k_9, AICC -244.1 without k_9), but produced negative rate constants when fit to 2D6 baculosomes data (Table 3). From simulations using the fit rate constants it was observed that inclusion of the k_9 pathway produced marginal visual differences in the fit to the data (Figure 5).

DMD Fast Forward. Published on October 22, 2019 as DOI: 10.1124/dmd.119.089268
This article has not been copyedited and formatted. The final version may differ from this version.

Discussion

A recurring obstacle for time-dependent inhibition parameterization has been the maintenance of linear enzyme inhibition after moderate to long preincubation periods, commonly resulting in the removal of any data that contains log-linear curvature. The classical PRA replot method relies on log-linear inactivation profiles in order to obtain k_{obs} points that are hyperbolic with respect to inhibitor concentration. As has been observed with MDMA in this work, the complete inactivation dataset likely contains information that can allow kineticists to make more specific predictions regarding enzyme inactivation rate, residual activity following inactivation, and DDI potential as a result of inhibition. Numerical curve fitting techniques are now allowing scientists to make use of data inaccessible to linear analyses such as the replot method and use non-steady-state information to hypothesize traditionally atypical kinetic mechanisms. Non-steady-state mechanisms such as the MAM and DEM have been applied to MDMA progress curves for initial inhibition analysis, and larger full TDI kinetic schemes have been used to corroborate the findings of recent spectral work with MDMA, suggesting a reversible inhibition mechanism.

Initial assessment of time dependent inhibition by MDMA was achieved with two numerical fittings of its progress curve. The rapid curvature in metabolite production reinforced the importance of non-steady-state techniques when interpreting the inhibition behavior of MDMA over long incubations. The progress curve approach was modeled with two mechanisms differing by their ability to account for residual activity after inhibition. The MAM was better able to model the terminal linear phase of the progress curve wherein, after a sharp decrease in metabolite production velocity, activity was still present. This result is indicative of an inhibition mechanism that does not permanently inactivate the protein. The k_{inact} analogues (k_5/k_3) obtained from these experiments quantify residual activity, which was found to be about three-fold greater

DMD Fast Forward. Published on October 22, 2019 as DOI: 10.1124/dmd.119.089268
This article has not been copyedited and formatted. The final version may differ from this version.

in HLM than recombinant 2D6. This may be due to the presence of other MDMA metabolizing proteins in HLM. The significant decrease in calculated K_I from the replot data in 2D6 baculosomes compared to HLM is also indicative of what is most likely contribution from non-2D6 MDMA metabolizers in microsomes. While this experiment allowed a quick first assessment of inhibition, more data-rich experiments were necessary to apply numerical models with greater kinetic complexity.

Full TDI experiments following the classical benchtop protocol of preincubation inhibition and secondary probe incubation phases were fit with two kinetic mechanisms that model reversible inhibition. In the recombinant 2D6 system, neither numerical model was able to properly characterize the data when the irreversible inhibition (k_9) pathway was included. Model fits with irreversible inactivation produced negative rate constants for k_8, a strong indicator that the model was fundamentally incorrect for the data. Conversely, both QI and EM models provided good solutions, and produced rate constants in the range of those estimated for the HLM QI and EM model fits.

In HLM both EM and QI mechanisms modeled the data well regardless of the presence of an irreversible inactivation event, though in both cases this event (k_9) was found to be relatively slow (0.0103 min^{-1} and 0.0104 min^{-1}, respectively). The difference between this and the 2D6 baculosome modeling may be a result of convolution due to other metabolizers in HLM acting on MDMA. It has been reported that in addition to 2D6, MDMA is a substrate of 2B6, 1A2, and 2C19 (Meyer *et al.*, 2008). It could also be a result of the increased potency of MDMA in 2D6 alone when compared to HLM, as the inactivation phase of the PRA plots is steeper in the recombinant system. The data in this case may not be rich enough to solve for a small permanent inactivation rate.

DMD Fast Forward. Published on October 22, 2019 as DOI: 10.1124/dmd.119.089268
This article has not been copyedited and formatted. The final version may differ from this version.

The kinetic analysis done in this work has been corroborated by the direct spectral evidence of reversible inactivation of MDMA in 2D6 recombinant systems reported previously (Rodgers *et al.*, 2018). In contrast to the first series of literature published indicating that MDMA is an irreversible MBI for 2D6, this body of work has provided evidence to support the conclusion that a slowly reversible mechanism is more likely. The classical steady-state method is incapable of distinguishing between slow reversibility and irreversible inhibition due to its mathematical assumptions and resulting data restrictions. Numerical methods in this case have proven to be useful for testing more detailed kinetic hypotheses *in silico*.

A secondary goal of this paper is to demonstrate the ability of numerical TDI kinetics to evaluate PRA plots with a greater degree of detail than has been done in the past with the replot method. In this case the inactivation data was nonlinear after brief incubations, suggesting that simple irreversible MBI formation was unlikely. The replot method is fundamentally incapable of incorporating any of the inhibition data for this type of inhibitor outside of its initial linear inactivation phase. Without a more detailed inspection, a resulting k_{inact} parameter would overpredict the *in vivo* scenario wherein the inhibitor would act on the protein for far longer than its initial linear time range (Yadav *et al.*, 2018). Assessment of the full range of inactivation data is necessary for better *in vitro in vivo* correlation and therefore DDI prediction. Further impact of characterizing the slow reversibility of a time dependent inhibitor comes by comparing the recovery of active enzyme to the enzyme's unaffected degradation rate. In a clinical study on the nonlinear kinetics of MDMA metabolism, the highest measured blood plasma concentrations of MDMA were reported to be 441.9-486.9µg/l (De La Torre *et al.*, 2000). The reversible numerical models described here allow us to predict that recovery of 80% of the protein's activity resulting from a similar concentration of MDMA would take approximately 25 hours.

This value is significantly faster than the resynthesis time of 2D6, which has been estimated to be 74 hours (Venkatakrishnan and Obach, 2005). While results from this type of PRA modeling can be used in concert with PBPK software to make *in vivo* clearance predictions, such studies remain an issue of future interest.

DMD Fast Forward. Published on October 22, 2019 as DOI: 10.1124/dmd.119.089268
This article has not been copyedited and formatted. The final version may differ from this version.

Authorship Contribution

Participated in research design: Rodgers, Jones

Conducted experiments: Rodgers

Performed data analysis: Rodgers

Wrote or contributed to the writing of the manuscript: Rodgers, Jones

References

A. Heydari, K. Rowland Yeo, M. S. Lennard, S. W. Ellis, G. T. Tucker AR-H (2004) Mechanism-Based Inactivation of CYP2D6 by Methylenedioxymethamphetamine. *Drug Metab Dispos* **32**:1213–1217.

Abbasi A, Paragas EM, Joswig-Jones CA, Rodgers JT, and Jones JP (2019) The Time-course of Aldehyde Oxidase and the Reason Why it is Nonlinear. *Drug Metab Dispos* doi: 10.1124/dmd.118.085787, American Society for Pharmacology and Experimental Therapeutics.

Antolino-Lobo I, Meulenbelt J, van den Berg M, and van Duursen MBM (2011) A mechanistic insight into 3,4-methylenedioxymethamphetamine ("ecstasy")-mediated hepatotoxicity. *Vet Q* **31**:193–205.

Atkinson A, Kenny JR, and Grime K (2005) Automated Assessment of Time-Dependent Inhibition of Human Cytochrome P450 Enzymes Using Liquid Chromatography-Tandem Mass Spectrometry Analysis. *Drug Metab Dispos* **33**:1637–47.

Barnaba C, Yadav J, Nagar S, Korzekwa K, and Jones JP (2016) Mechanism-Based Inhibition of CYP3A4 by Podophyllotoxin: Aging of an Intermediate Is Important for in Vitro/in Vivo Correlations. *Mol Pharm* **13**:2833–2843.

Bastos ML, Carvalho M, Milhazes N, Remiao F, Borges F, Fernandes E, Amado F, Monks TJ, and Carvalho F (2004) Hepatotoxicity of 3,4-methylenedioxyamphetamine and alpha-methyldopamine in isolated rat hepatocytes: formation of glutathione conjugates. *Arch Toxicol* **78**:16–24, Springer-Verlag.

Burt HJ, Pertinez H, Sä C, Collins C, Hyland R, Houston JB, and Galetin A (2012) Progress

Curve Mechanistic Modeling Approach for Assessing Time-Dependent Inhibition of CYP3A4. *Drug Metab Dispos* **40**:1658–1667.

Cao W, De EM, and Cruz L (2013) Quantitative full time course analysis of nonlinear enzyme cycling kinetics. *Sci Rep* **3**:2658.

Cleland W (1975) Partition analysis and concept of net rate constants as tools in enzyme kinetics. *Biochemistry* **14**:3220–3224, American Chemical Society.

De La Torre R, Farré M, Ortuño J, Mas M, Brenneisen R, Roset PN, Segura J, and Cami J (2000) Non-linear pharmacokinetics of MDMA ('ecstasy') in humans. *Br J Clin Pharmacol* **49**:104–109.

De La Torre R, Farré M, Roset PN, Pizarro N, Abanades S, Segura M, Segura J, and Camí J (2004) Human Pharmacology of MDMA Pharmacokinetics, Metabolism, and Disposition. *Ther Drug Monit* **26**:137–144.

Dowling GP, McDonough ET, and Bost RO (1987) "Eve" and "Ecstasy." *JAMA* **257**:1615, American Medical Association.

Grimm SW, Einolf HJ, Hall SD, He K, Lim H, Ling KJ, Lu C, Nomeir AA, Seibert E, Skordos KW, Tonn GR, Horn R Van, Wang RW, Wong YN, Yang TJ, and Obach RS (2009) The Conduct of in Vitro Studies to Address Time-Dependent Inhibition of Drug- Metabolizing Enzymes : A Perspective ... The Conduct of in Vitro Studies to Address Time-Dependent Inhibition of Drug-Metabolizing Enzymes : A Perspective of the Pharmaceutical. *Drug Metab Dispos* **37**:1355–1370.

Harrington RD, Woodward JA, Hooton TM, and Horn JR (1999) Life-Threatening Interactions

Between HIV-1 Protease Inhibitors and the Illicit Drugs MDMA and γ-Hydroxybutyrate. *Arch Intern Med* **159**:2221–2224, American Medical Association.

Korzekwa K, Tweedie D, Argikar UA, Whitcher-Johnstone A, Bell L, Bickford S, and Nagar S (2014) A Numerical Method for Analysis of In Vitro Time-Dependent Inhibition Data. Part 2. Application to Experimental Data. *Drug Metab Dispos* **42**:1587–1595.

Meyer MR, Peters FT, and Maurer HH (2008) The Role of Human Hepatic Cytochrome P450 Isozymes in the Metabolism of Racemic 3 , 4-Methylenedioxy- Methamphetamine and Its Enantiomers. *Drug Metab Dispos* **36**:2345–2354.

Michaels S, and Wang MZ (2014) The revised human liver cytochrome P450 "Pie": absolute protein quantification of CYP4F and CYP3A enzymes using targeted quantitative proteomics. *Drug Metab Dispos* **42**:1241–51, American Society for Pharmacology and Experimental Therapeutics.

Nagar S, Jones JP, and Korzekwa K (2014) A Numerical Method for Analysis of In Vitro Time-dependent Inhibition Data. Part I. Theoretical Considerations. *Drug Metab Dispos* **42**:1575–86.

Orr STM, Ripp SL, Ballard TE, Henderson JL, Scott DO, Obach RS, Sun H, and Kalgutkar AS (2012) Mechanism-Based Inactivation (MBI) of Cytochrome P450 Enzymes: Structure–Activity Relationships and Discovery Strategies To Mitigate Drug–Drug Interaction Risks. *J Med Chem* **55**:4896–4933, American Chemical Society.

Rodgers JT, Davydova NY, Paragas EM, Jones JP, and Davydov DR (2018) Kinetic mechanism of time-dependent inhibition of CYP2D6 by 3,4-methylenedioxymethamphetamine (MDMA): Functional heterogeneity of the enzyme and the reversibility of its inactivation.

Biochem Pharmacol **156**:86–98, Elsevier.

Screaton GR, Cairns HS, Sarner M, Singer M, Thrasher A, and Cohen SL (1992) Hyperpyrexia and rhabdomyolysis after MDMA ("ecstasy") abuse. *Lancet* **339**:677–678, Elsevier.

Silverman RB (1995) Mechanism-based enzyme inactivators. *Methods Enzymol* **249**:240–283, Academic Press.

Soars MG, McGinnity DF, Grime K, and Riley RJ (2007) The pivotal role of hepatocytes in drug discovery. *Chem Biol Interact* **168**:2–15, Elsevier.

Takakusa H, Wahlin MD, Zhao C, Hanson KL, New LS, Chan ECY, and Nelson SD (2011) Metabolic intermediate complex formation of human cytochrome P450 3A4 by lapatinib. *Drug Metab Dispos* **39**:1022–30, American Society for Pharmacology and Experimental Therapeutics.

Van LM, Heydari A, Yang J, Hargreaves J, Rowland-Yeo K, Lennard MS, Tucker GT, and Rostami-Hodjegan A (2006) The impact of experimental design on assessing mechanism-based inactivation of CYP2D6 by MDMA (Ecstasy). *J Psychopharmacol* **20**:834–841.

Van LM, Swales J, Hammond C, Wilson C, Hargreaves JA, and Rostami-Hodjegan A (2007) Kinetics of the time-dependent inactivation of CYP2D6 in cryopreserved human hepatocytes by methylenedioxymethamphetamine (MDMA). *Eur J Pharm Sci* **31**:53–61, Elsevier.

VandenBrink BM, and Isoherranen N (2010) The role of metabolites in predicting drug-drug interactions: focus on irreversible cytochrome P450 inhibition. *Curr Opin Drug Discov Devel* **13**:66–77, NIH Public Access.

Venkatakrishnan K, and Obach RS (2005) In vitro-in vivo extrapolation of CYP2D6 inactivation by paroxetine: prediction of nonstationary pharmacokinetics and drug interaction magnitude. *Drug Metab Dispos* **33**:845–52, American Society for Pharmacology and Experimental Therapeutics.

Wienkers LC, and Heath TG (2005) Predicting in vivo drug interactions from in vitro drug discovery data. *Nat Rev Drug Discov* **4**:825–833.

Yadav J, Korzekwa K, and Nagar S (2018) Improved Predictions of Drug–Drug Interactions Mediated by Time-Dependent Inhibition of CYP3A. *Mol Pharm* **15**:1979–1995, American Chemical Society.

Zanger UM, and Schwab M (2013) Cytochrome P450 enzymes in drug metabolism: Regulation of gene expression, enzyme activities, and impact of genetic variation. *Pharmacol Ther* **138**:103–141, Pergamon.

DMD Fast Forward. Published on October 22, 2019 as DOI: 10.1124/dmd.119.089268
This article has not been copyedited and formatted. The final version may differ from this version.

Footnotes

This work was supported by National Institute of Health [Grant R01-GM114369]

DMD Fast Forward. Published on October 22, 2019 as DOI: 10.1124/dmd.119.089268
This article has not been copyedited and formatted. The final version may differ from this version.

Figure Legends

Figure 1. Progress curve modeling according to the Modified Activity Model (Left) and Dead Enzyme Model (Right). Dihydroxy metabolite formation measured in HLM (A, B) and 2D6 Baculosomes (C,D). The Dead Enzyme Models contains MDMA turnover to the measured product (P) with irreversible inactivation to form E*S via k_4. In the Modified Activity Model, k_4 converts the protein to a less active form (E*) which models any remaining activity upon inhibition due to S. The remaining activity is described by the second turnover rate k_5.

Figure 2. Classical TDI experiments for MDMA inactivation of HLM (A,B) and 2D6 baculosomes (C,D). Remaining-activity measured by dextromethorphan datasets are truncated to include on the log-linear points for assessment by the replot method. Slopes are replot against inhibitor concentration to obtain steady-state inactivation parameters.

Figure 3: QI Model (left), Equilibrium Model (right). Both models were tested in the presence and absence of the irreversible inactivation (k_9) pathway. Models include probe substrate (S) turnover to measured product (P, dextrorphan). Inhibition is represented in the vertical pathway with MDMA (I) binding to form EI. Enzyme inactivation is accomplished via conversion to E2, where the complex is permanently inactivated via k_9. Recovery in the EM model occurs via the k_7/k_8 equilibrium to reform EI. In the QI model recovery occurs through the single micro rate k_7, and unbound E and I are regenerated.

Figure 4. Fits of HLM PRA plots: EM model without k_9 (A,B); EM model with k_9 (C,D); QI model without k_9 (E,F); QI model with k_9 (G,H).

Figure 5. Fits of 2D6 Baculosomes PRA plots: EM model without k_9 (A,B); QI model without k_9 (C,D).

DMD Fast Forward. Published on October 22, 2019 as DOI: 10.1124/dmd.119.089268
This article has not been copyedited and formatted. The final version may differ from this version.

Table 1. Rate constant outputs from numerical progress curve analysis.

Rate Constant (min^{-1})	HLM		2D6 Baculosomes	
	DEM	MAM	DEM	MAM
k_3	10.43 ± 0.87	13.01 ± 1.31	91.97 ± 10.71	112.5 ± 13.6
k_4	0.448 ± 0.045	0.721 ± 0.109	1.28 ± 0.16	1.85 ± 0.26
k_5	–	0.461 ± 0.106	–	1.28 ± 0.23

DMD Fast Forward. Published on October 22, 2019 as DOI: 10.1124/dmd.119.089268
This article has not been copyedited and formatted. The final version may differ from this version.

Table 2. Rate constant outputs from two numerical TDI models for HLM data. Each is tested in the presence and absence of the irreversible inactivation event (k_9).

Rate Constant (min^{-1})	EM		QI	
	Irreversible	Reversible	Irreversible	Reversible
k_3	6.291 ± 0.129	6.270 ± 0.112	6.294 ± 0.118	6.270 ± 0.126
k_6	0.3800 ± 0.0642	0.3411 ± 0.0024	0.3833 ± 0.0634	0.3425 ± 0.0359
k_7	0.0538 ± 0.0174	0.0406 ± 0.0026	0.0545 ± 0.0176	0.0406 ± 0.0049
k_8	0.0118 ± 0.0130	0.0102 ± 0.0020	0.0126 ± 0.0134	0.0103 ± 0.0020
k_9	0.0103 ± 0.0020	–	0.0104 ± 0.0013	–

DMD Fast Forward. Published on October 22, 2019 as DOI: 10.1124/dmd.119.089268
This article has not been copyedited and formatted. The final version may differ from this version.

Table 3. Rate constant estimates from numerical modeling of TDI data in 2D6 baculosomes.

Rate Constant (min^{-1})	EM		QI	
	Irreversible[a]	Reversible	Irreversible[a]	Reversible
k_3	22.61 ± 0.317	22.63 ± 0.310	22.61 ± 0.32	22.63 ± 0.31
k_6	1.650 ± 0.149	1.693 ± 0.134	1.648 ± 0.148	1.692 ± 0.134
k_7	0.0559 ± 0.0056	0.0586 ± 0.0029	0.0556 ± 0.0056	0.0584 ± 0.0029
k_8	-0.0023 ± 0.0040	0.0240 ± 0.0017	-0.0022 ± 0.0040	0.0240 ± 0.0017
k_9	0.0239 ± 0.0017	–	0.0239 ± 0.0017	–

[a]Entire set of model fits invalidated by negative value output.

DMD Fast Forward. Published on October 22, 2019 as DOI: 10.1124/dmd.119.089268
This article has not been copyedited and formatted. The final version may differ from this version.

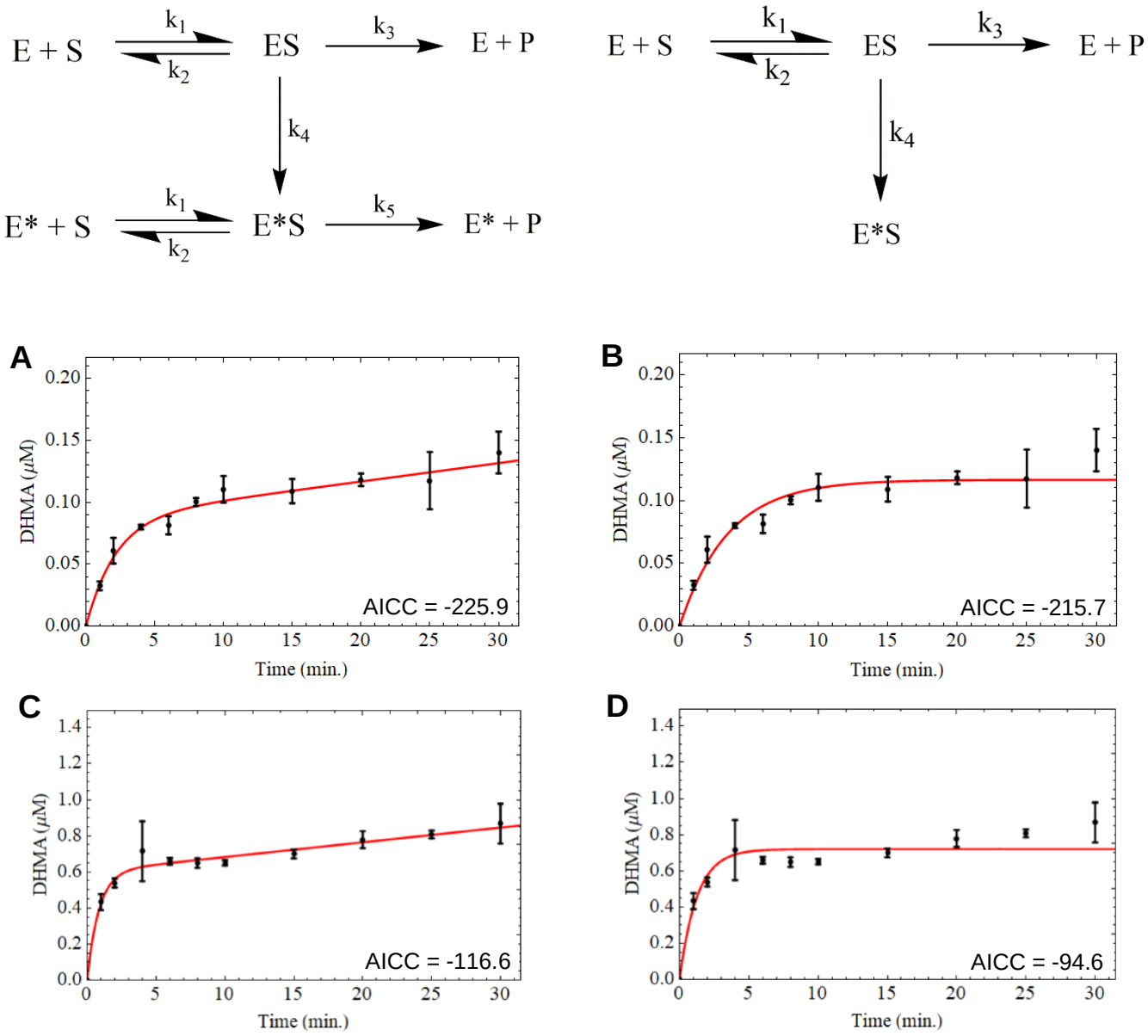

Figure 1.

DMD Fast Forward. Published on October 22, 2019 as DOI: 10.1124/dmd.119.089268
This article has not been copyedited and formatted. The final version may differ from this version.

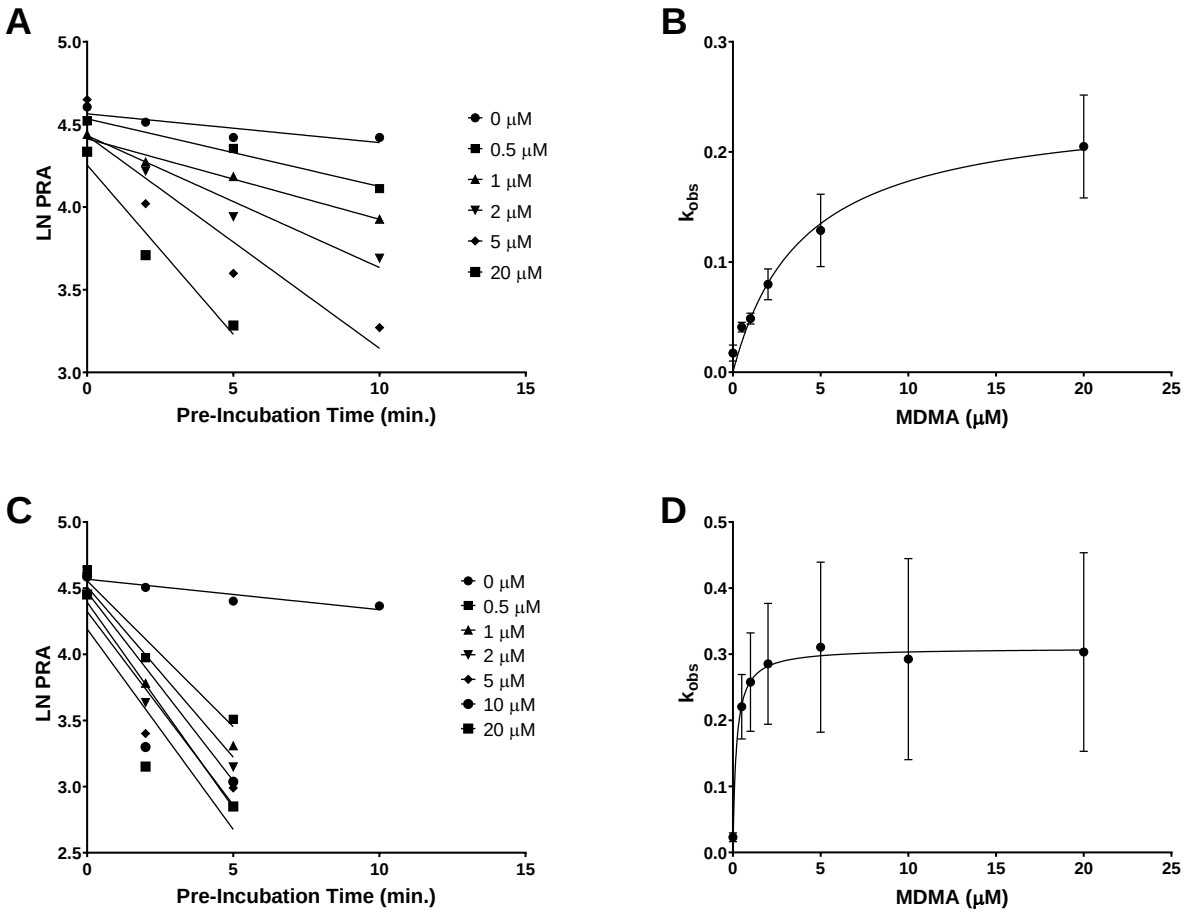

Figure 2.

DMD Fast Forward. Published on October 22, 2019 as DOI: 10.1124/dmd.119.089268
This article has not been copyedited and formatted. The final version may differ from this version.

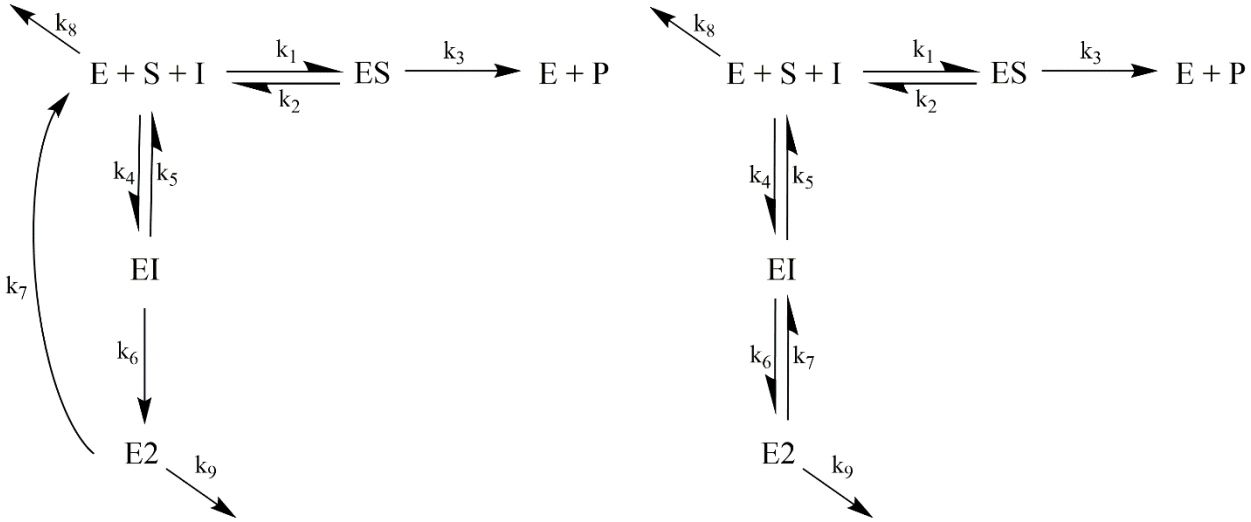

Figure 3.

DMD Fast Forward. Published on October 22, 2019 as DOI: 10.1124/dmd.119.089268
This article has not been copyedited and formatted. The final version may differ from this version.

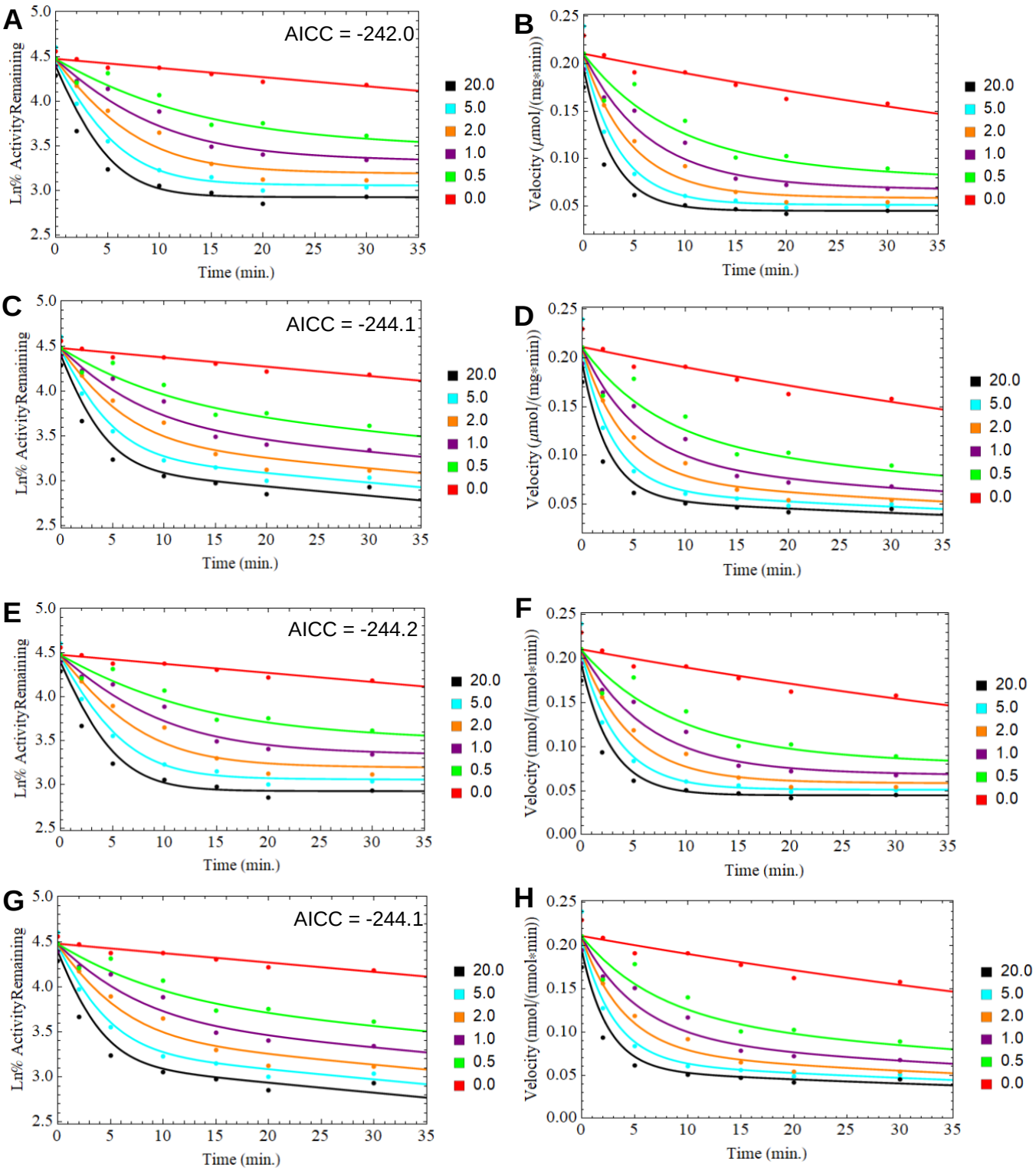

Figure 4.

DMD Fast Forward. Published on October 22, 2019 as DOI: 10.1124/dmd.119.089268
This article has not been copyedited and formatted. The final version may differ from this version.

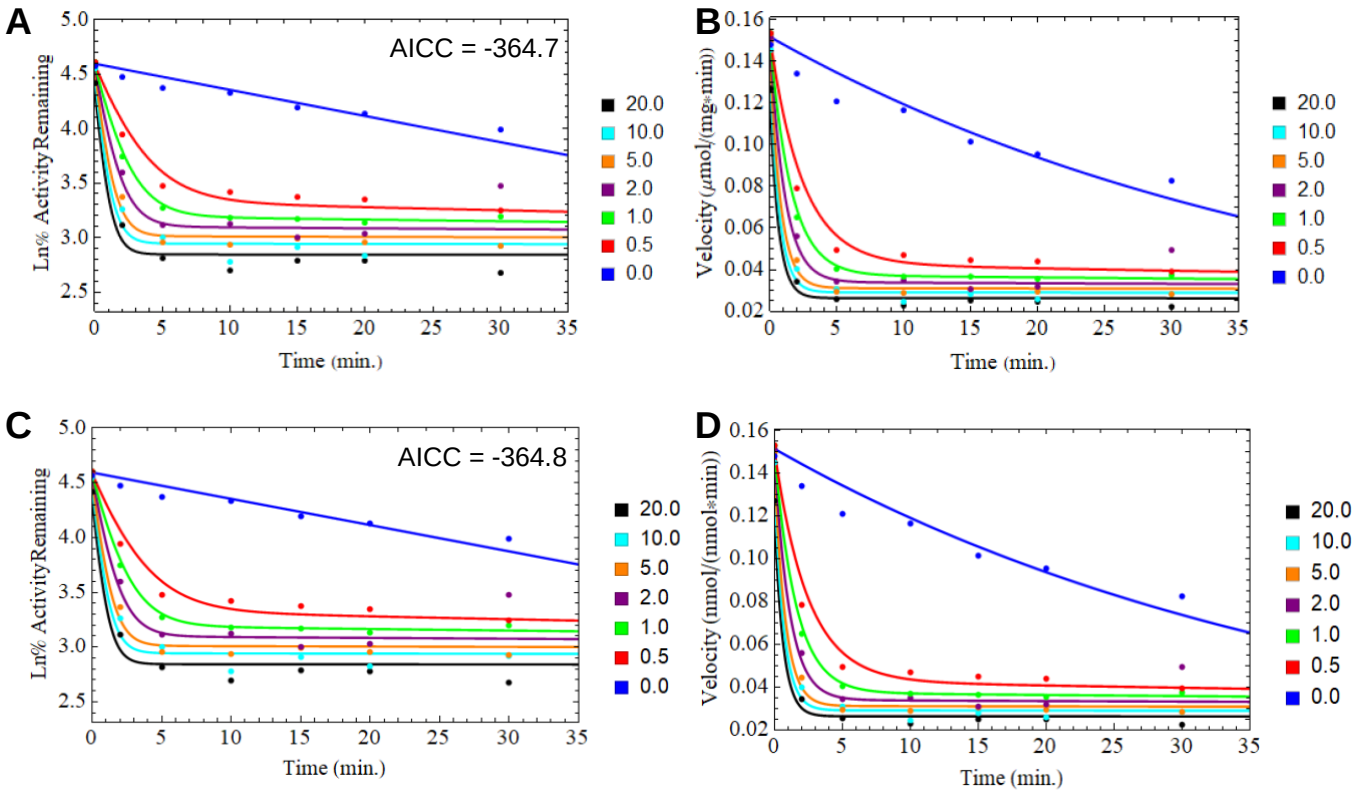

Figure 5.